Environment Protection Engineering

Vol. 39 2013 No. 3

DOI: 10.5277/epe130303

LEI SONG[1], TIANHU CHEN[1], DONG CHEN[1], YI CHEN[1], JINGJING XIE[1], HAIBO LIU[1]

CATALYTIC DECOMPOSITION OF TOLUENE OVER $La_{1-x}Sr_xMnO_3$/PALYGORSKITE SYNTHESIZED CATALYSTS

Palygorskite (PG) supported $La_{1-x}Sr_xMnO_3$ catalysts were fabricated by coprecipitation. The catalysts were characterized by X-ray diffraction (XRD), transmission electron microscopy (TEM), specific surface area (SSA) and H_2 temperature programmed reduction (H_2-TPR). Catalytic activity for VOCs was examined by using toluene as a model compound. The results show that the surface area as well as mechanical strength of catalysts increase substantially after catalysts loaded in PG. XRD patterns show that after calcination at 700 °C, PG as a support in 9% $LaMnO_3$/PG and 9% $La_{0.7}Sr_{0.3}MnO_3$/PG was transformed into amorphous phase and the morphology was not destroyed. It was well established that the main reductive components are factually Mn(III) or Mn(IV) oxides in catalysts based on the results of TPR. It was also found that Mn(IV) increases while Mn(III) reduces responding with the increasing amount of Sr. Toluene conversion rate of as-prepared μ% $La_{1-x}Sr_xMnO_3$/PG increases with the increasing values of x and μ when x = 0–0.3 and μ = 3–9%. Toluene can be converted completely at 285 °C by 9% $La_{0.7}Sr_{0.3}MnO_3$/PG catalyst while no significant change was observed after addition on the doping and loading amount of Sr. During a 100 h stability experiment of 9% $La_{0.7}Sr_{0.3}MnO_3$/PG catalyst, toluene removal was found to be above 95%.

1. INTRODUCTION

Volatile organic compounds (VOCs) are detrimental to human health. In order to make the removal reaction economically competitive, it is necessary to explore higher active catalysts to be used at low temperatures [1–5]. The efficiency of such technology is determined by the activity and stability of the catalyst. Currently, various kinds of catalysts such as supported noble metals and base metal oxides have been investigated widely for the catalytic combustion of VOCs [6–10]. Among them, supported noble metals have been generally regarded as the most desirable catalysts, in terms of their catalytic activity, selectivity and stability for catalytic oxidation. However, their ap-

[1]School of Resources and Environmental Engineering, Hefei University of Technology, Hefei 230009, Anhui, China, corresponding author Tianhu Chen, e-mail: chentianhu168@vip.sina.com

plications are limited due to high costs and problems related to sintering and volatility. Among the base metal oxides, perovskite-type oxide (ABO_3) is regarded as the most promising catalyst for the complete oxidation of hydrocarbons and oxygenates [11, 12]. Perovskites with lanthanum in A sites and transition metals in B sites ($LaBO_3$, B = Mn, Co, Fe, Ni) have attracted much attention. Particularly, partial substitution of lanthanum in $LaMnO_3$ by Sr, Ce, Hf, Ag, or Ca was reported to enhance the catalytic activity in full oxidation [13-19]. Palygorskite is a magnesium aluminium phyllosilicate with general chemical formula $Mg_5Si_8O_{20}(OH)_2(H_2O)_4{\cdot}4H_2O$. In TEM images, its microstructure is rod-like or fibrous. Abundant reserve of palygorskite is found in Jiangsu and Anhui province of China. This kind of mineral is widely used because of nano-sized properties, low price, high strength and large surface area. Even though there are lots of reports on mineralogical properties and application of palygorskite in China [20–23], the application of palygorskite as the catalyst support for VOCs conversion has not yet been investigated. In this work, a series of catalysts were prepared when the perovskite-type active component was loaded on palygorskite.

2. EXPERIMENTAL

Catalyst preparation. Palygorskite clay powder (Mingguang City of Anhui Province, Guanshan palygorskite clay mine) with the particle size smaller than 70 μm was obtained by extrusion, drying, crushing and screening. It consisted of SiO_2, Al_2O_3, MgO, Fe_2O_3 and FeO [24]. The catalysts were fabricated by the co-precipitation method. 600 cm^3 of deionized water was added to a 1000 cm^3 baker containing appropriate proportion of $La(NO_3)_3{\cdot}6H_2O$, $Sr(NO_3)_2$ and $Mn(NO_3)_2$. Consecutively, a certain amount of palygorskite powder was added under stirring for 2 h. Then ammonia was dropped to the mixture at a certain stirring speed for adjusting pH to 10. The suspension obtained was firstly washed with deionized water, and then dried overnight at 105 °C. The dried samples were calcinated in a muffle furnace at 700 °C for 2 h. Finally, the catalysts were crushed and sieved to 40–60 mesh particles in order to get perovskite of various quality. Obtained samples were denoted by μ% $La_{1-x}Sr_xMnO_3$/PG, and μ means the content of $La_{1-x}Sr_xMnO_3$ perovskite in the PG.

Catalysts characterization. X-ray diffraction (XRD) patterns were recorded on a Rigaku D/max-rB X-ray diffractometer. All samples were examined at 40 kV and 100 mA using CuK_α radiation, full XRD patterns were recorded in the range of 3–80° at the scan speed of 5 deg·min^{-1}. JEM-2100 high-resolution transmission electron microscopy (TEM) was used to observe the morphology of catalysts. Specific surface areas of catalyst were determined by N_2 adsorption at 77 K on a Quantachrome Nova 3000e analyzer. The sample was degassed for 6 h at 300 °C before N_2 adsorption. The specific surface area was obtained by the BET equation. The pore volume was evaluat-

ed from N_2 uptake at a relative N_2 pressure of $p/p_0 = 0.975$. The particle pressure in catalysts was measured with a KC-2A stress test machine (Jiangyan Yinghe, China). Hydrogen temperature programmed reduction (H_2-TPR) experiments were carried out in a self-made equipment. 100 mg of catalyst was loaded in a quartz tube with air pretreatment for 1 h at 300 °C. Then the catalyst was heated under a 5% H_2/Ar gas mixture, at the heating rate of 10 °C·min^{-1} to 750 °C. The effluent gas was analyzed by means of an on-line mass spectrometer (MS, Hiden QIC-20).

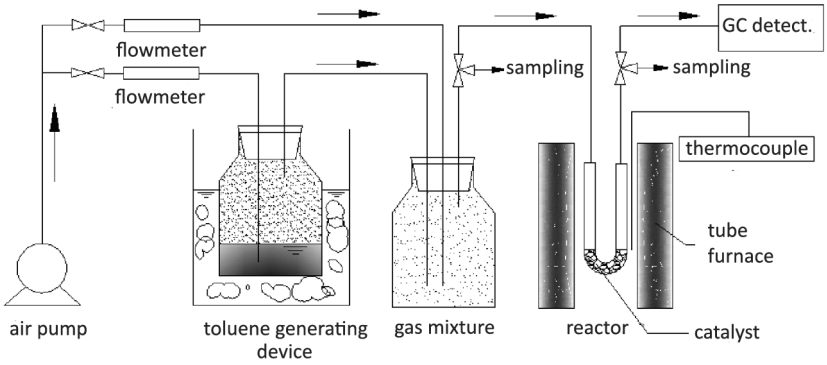

Fig. 1. Apparatus for the catalytic activity estimation

Catalyst activity. Catalyst activity tests were conducted in a laboratory scale, with a packed-bed flow reactor made of U shape quartz tube (i.d. = 6 mm), vertical furnace and supporting catalyst (Fig. 1). Air was divided into two ways. In one way, air was bubbled under the toluene liquid surface to obtain toluene vapor, the other way for dilution gas. The gas was fed into the catalytic oxidation reactor after being mixed in a mixing cylinder. By adjusting the flows of two-way gas, toluene concentration was kept constant at 3790 mg/m^3, and the gas hourly space velocity (GHSV) was 7200 h^{-1}. The inlet and outlet toluene concentrations were detected by a Shimadzu GC with a FID detector (GC-2010), the conversion of toluene was measured three times after each experiment, taking its mean value as the experimental result.

3. RESULTS AND DISCUSSION

3.1. RESULT OF CATALYST CHARACTERIZATION

Table 1 shows the specific surface area and compressive strength of various catalysts. Crystalline $La_{0.7}Sr_{0.3}MnO_3$ perovskite has not been detected due to the low compressive strength while its surface area is only 4.6 m^2/g. However after loading on PG, it displays higher surface area. The corresponding increase is ascribed as a large number of mesopores which can be piled among one-dimension rod nanocrystallites of raw

palygorskite. It can improve catalytic performance by scattering active components. After loading of active component and calcination, the compressive strength of the catalyst increases obviously compared to unloaded active component. Although the folded pores happen inside PG, surface area of catalyst remains higher than 75 m^2/g after calcination at 700 °C [25]. The increase of compressive strength and BET specific surface area in catalysts is expected to improve the catalytic performance in the reaction.

Table 1

Specific surface area and compressive strength of various catalysts

Catalyst/PG	BET surface area [m^2/g]	Compressive strength [N]
	148.3	21.6
3% $La_{0.7}Sr_{0.3}MnO_3$/PG	85.9	21.3
5% $La_{0.7}Sr_{0.3}MnO_3$/PG	82.4	18.1
7% $La_{0.7}Sr_{0.3}MnO_3$/PG	81.9	17.8
9% $La_{0.7}Sr_{0.3}MnO_3$/PG	80.5	17.2
11% $La_{0.7}Sr_{0.3}MnO_3$/PG	75.3	16.6
$La_{0.7}Sr_{0.3}MnO_3$	4.6	—
9% $LaMnO_3$/PG	79.6	16.8
9% $La_{0.9}Sr_{0.1}MnO_3$/PG	83.2	17.1
9% $La_{0.8}Sr_{0.2}MnO_3$/PG	80.7	17.0
9% $La_{0.6}Sr_{0.4}MnO_3$/PG	78.1	17.5

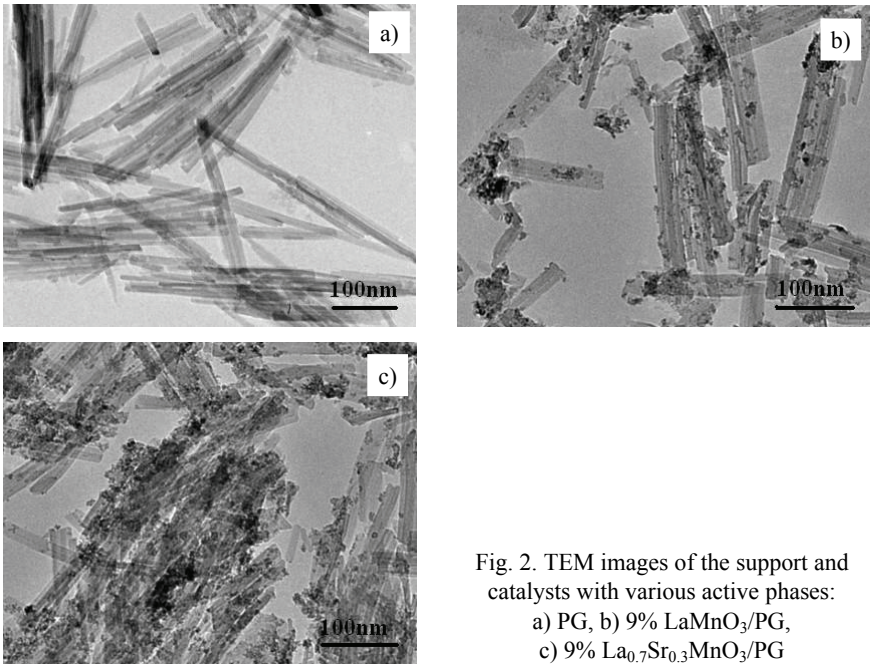

Fig. 2. TEM images of the support and catalysts with various active phases: a) PG, b) 9% $LaMnO_3$/PG, c) 9% $La_{0.7}Sr_{0.3}MnO_3$/PG

In Figure 2a, raw PG shows a rod-like structure. Figure 2b corresponds to the catalyst of 9% $LaMnO_3$/PG, and in Fig. 2c 9% $La_{0.7}Sr_{0.3}MnO_3$/PG is shown. From Figures 2b and 2c, it is evident that loaded active components of two catalysts after calcination are well dispersed on the PG surface with a particle size of 5 nm. Both catalysts in Figs. 2b and 2c have a similar rod-like structure as raw PG. Alternatively, the loaded active components can restrain the sinterization or contraction of the PG calcination.

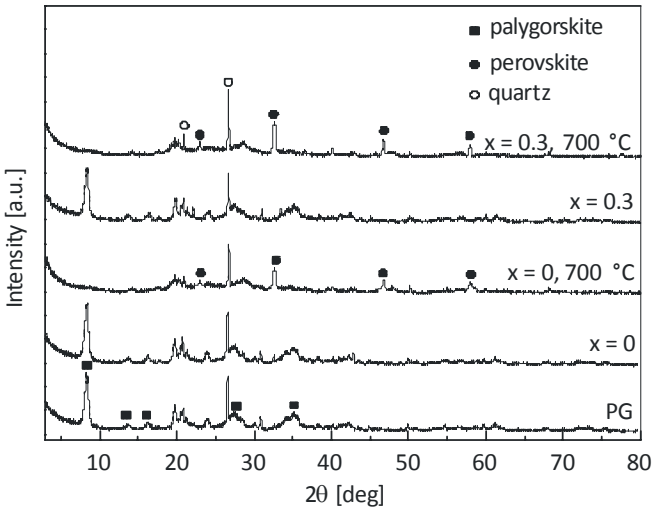

Fig. 3. XRD patterns of various substitutions of Sr in 9% $La_{1-x}Sr_xMnO_3$/PG

Figure 3 shows XRD patterns of La, Sr-substituted 9% $La_{1-x}Sr_xMnO_3$/PG. The peaks in patterns are mainly assigned to palygorskite in both catalysts as 9% $LaMnO_3$/PG and 9% $La_{0.7}Sr_{0.3}MnO_3$/PG. It is also confirmed that the amorphous active components are highly dispersed at the palygorskite surface. After calcination at 700 °C, significant diffraction peaks appear at 2θ = 23.0°, 32.6°, 46.7°, 58.0° in the catalysts, corresponding to La-Mn perovskite crystal structure after high temperature calcination. At the same time, the palygorskite peaks disappear after calcination, it is also noted that palygorskite appears as an amorphous phase. After the catalyst calcination, it shows only peaks assigned to the perovskite phase and PG background in the corresponding pattern. The corresponding peaks of lanthanum and manganese oxides do not appear, which shows that proper addition can make strontium partly replaced by lanthanum in the perovskite structure. The formation of the perovskite and doping will enhance the efficiency of catalytic oxidation [26].

In the catalytic oxidation of toluene, the redox properties of catalyst are closely related to the catalytic activity. The temperature-programmed hydrogen reduction (H_2-TPR) is a common measurement to find out the component type of reduction and the relative content of the catalyst. Figure 4 shows H_2-TPR profiles of La, Sr-

substituted 9% $La_{1-x}Sr_xMnO_3$/PG. As shown in the figure, no significant hydrogen consumption peaks can be found in the profile of PG. But perovskite, 9% $La_{1-x}Sr_xMnO_3$/PG has two reduction peaks, one located at ca. 348 °C and the other at ca. 401 °C.

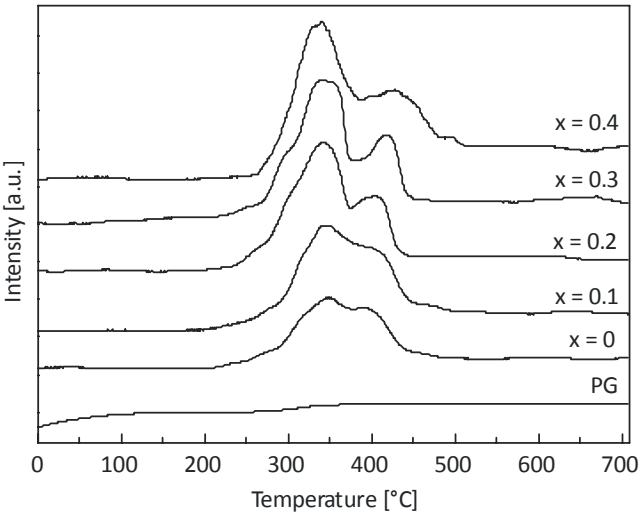

Fig. 4. H_2-TPR profiles of different substitution quantity of Sr in 9% $La_{1-x}Sr_xMnO_3$/PG

Based on the report of Walter [27, 28], it is inferred that the first reduction peak should be attributed to the reduction of Mn(IV) to Mn(III), and the second one may be assigned to reduction of Mn(III). In addition, it can be seen that with the increasing amount of Sr, the amount of Mn(IV), increases with a decreasing amount of Mn(III). It can be concluded that the substitution of rare earth metal will enhance the yield of reductive component such as Mn(IV).

3.2. ANALYSIS OF THE TOLUENE CONVERSION RATE

The catalytic activity of toluene oxidation are usually estimated by three performance indices: $T_{10\%}$ – the ignition temperature when conversion of toluene is 10%, $T_{50\%}$ – the semi-complete conversion temperature when conversion of toluene is 50% and $T_{99\%}$ – the temperature when 99% of toluene has been converted. The lower conversion temperature is better for the catalytic activity of catalysts, and the primary object in catalyst activity is the temperature of the complete conversion on toluene ($T_{99\%}$). The three performance indices are listed in Tables 2 and 3. As shown in Fig. 5, $T_{99\%}$ of 9% $La_{1-x}Sr_xMnO_3$/PG is 339°, $x = 0$, and with the increasing amount of Sr, the toluene conversion rate increased gradually. When $x = 0.3$, the temperature of 99% toluene conversion ($T_{99\%}$) for 9% $La_{1-x}Sr_xMnO_3$/PG reached 285 °C, by 54 °C higher

than that of the undoped catalyst. But there is almost no change in catalytic activity while additional Sr is doped, for example, $x = 0.4$. It is assigned to the replacement of La ions by smaller Sr ions. Because of the difference of the ionic radius and valence, the migration path of oxygen in the lattice increases relatively, which could reduce the oxygen proliferation in the lattice due to effective steric hindrance and increase the oxygen activity, in order to promote the catalytic oxidation reaction. But excessive addition of Sr would be detrimental for perovskite crystal growth and the catalyst activity. The data obtained suggest that 0.3 is the favorite amount of doped Sr in the catalytic activity experiments.

Table 2

Temperatures [°C] of 10%, 50% and 99% toluene conversion
for various substitution quantities of Sr in $La_{1-x}Sr_xMnO_3$/PG catalysts

Conversion	Catalyst content				
	$X = 0.4$	$X = 0.3$	$X = 0.2$	$X = 0.1$	$X = 0$
10%	221	241	261	264	283
50%	254	256	275	287	307
99%	293	285	314	318	339

Table 3

Temperatures [°C] of 10%, 50% and 99% toluene conversion
of various contents of $La_{1-x}Sr_xMnO_3$/PG catalysts and blank sample

Conversion	Catalyst contents						
	3%	5%	7%	9%	11%	PG	Blank
10%	283	283	263	241	242	326	–
50%	309	304	285	256	254	–	–
99%	339	339	319	285	296	–	–

After the amount of Sr was determined, investigation on the amount of $La_{0.7}Sr_{0.3}MnO_3$ perovskite loading on PG for the toluene conversion was performed. In Figure 6, the conversion rate of toluene is shown in function of the amount of catalyst loading on PG ranging from 0.03 to 0.11. When catalyst loading is 0.05, $T_{99\%}$ is 339 °C. While the loading increases to 0.07, $T_{99\%}$ decreases to 319 °C. The 9% loading of PG will cause 98.6% toluene conversion at 280 °C. However, when the loading amount is 11%, the change of toluene conversion rate is lower. It could be ascribed to the fact that the excessive amount of perovskite on the surface of PG support accumulates so that it reduces the contact area of the active component and toluene molecules. In other words, the catalytic activity is no longer improved with more loading amount of catalysts.

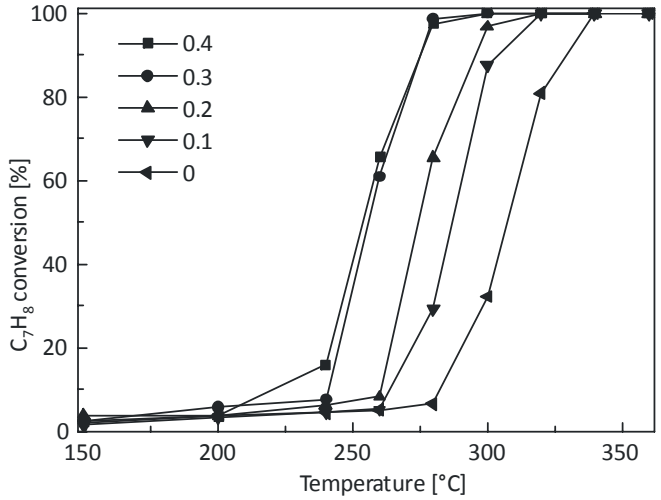

Fig. 5. Toluene conversions conducted on various amounts of Sr in 9% $La_{1-x}Sr_xMnO_3$/PG catalysts at various temperatures

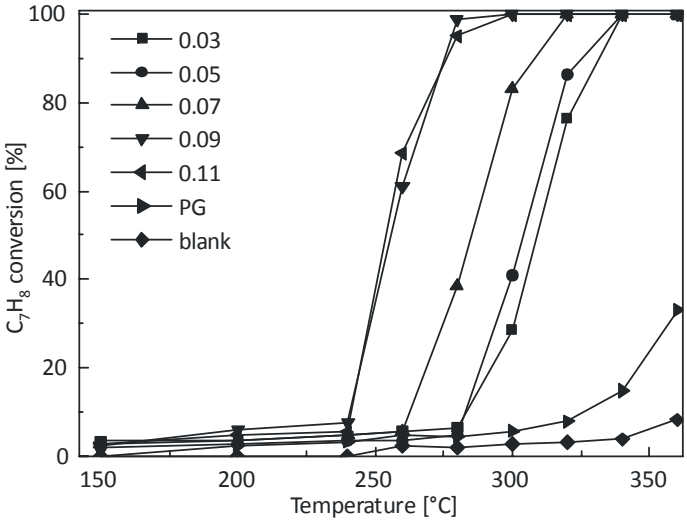

Fig. 6. Toluene conversions conducted on various supported amounts of $La_{0.7}Sr_{0.3}MnO_3$/PG catalysts and blank sample at various temperatures

3.3. ANALYSIS OF THE CATALYST STABILITY

In a preliminary test of stability of 9% $La_{0.7}Sr_{0.3}MnO_3$/PG, the toluene conversion rate in 100 h was tested. The catalytic oxidation reaction temperature was held at 280 °C, and the results are shown in Fig. 7. In the stability experiment, the catalyst maintained a high toluene conversion rate of more than 95%. At the end of reaction, the catalyst

particles can be recycled completely. Furthermore, no significant carbon deposition is observed at the catalyst surface as well as in the reactor.

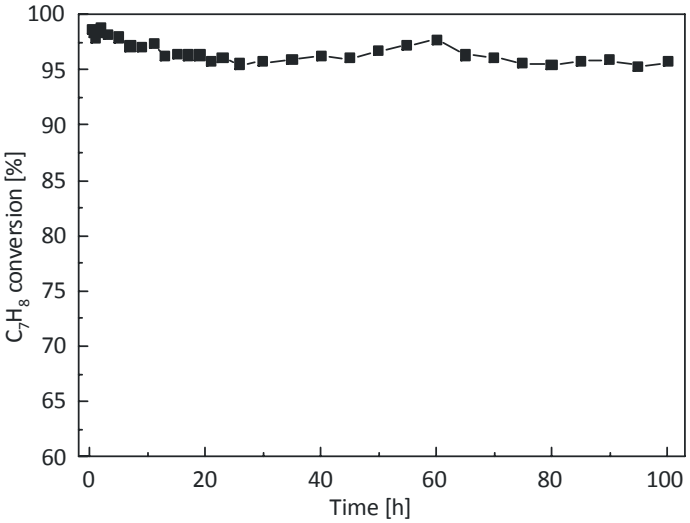

Fig. 7. Stability experiment of 9% $La_{0.7}Sr_{0.3}MnO_3$/PG catalyst during 100 h test at 280 °C

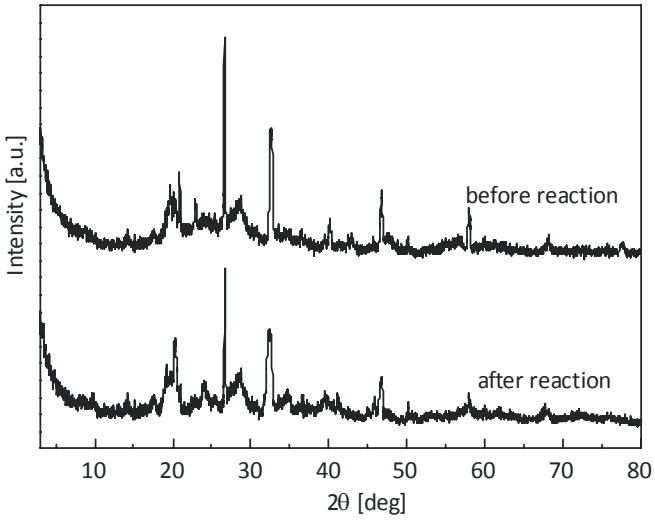

Fig. 8. XRD patterns of fresh and used 9% $La_{0.7}Sr_{0.3}MnO_3$/PG catalyst

Figure 8 presents XRD patterns of 9% $La_{0.7}Sr_{0.3}MnO_3$/PG before and after reaction. From the figure, the presence of lanthanum manganese perovskite is still clear in the catalyst whenever before and after the reaction. The relative intensity of each peak

does not change significantly, indicating that the crystalline phase and structure of the catalyst after 100 h of continuous catalytic oxidation exhibit a sufficient long-term stability. Lack of significant reactions such as sinterization of the active component or of the support demonstrate high structural stability and promising catalytic activity of the catalyst.

4. CONCLUSIONS

Perovskite-type $La_{1-x}Sr_xMnO_3$ catalysts can be fabricated by co-precipitation. Their surface areas and compressive strength increase substantially after loading on PG. The active component shows a uniform nanostructure. XRD patterns show that after calcination at 700 °C, in both catalysts, 9% $LaMnO_3$/PG and 9% $La_{0.7}Sr_{0.3}MnO_3$/PG, the PG support is transformed into amorphous phase while the rod-like morphology still maintains. The active component turns from the amorphous form to a certain degree of crystallization. The results of TPR inform that 9% of $La_{1-x}Sr_xMnO_3$ catalyst can restore the main component of Mn(III), and Mn(IV). It was also found that Mn(IV) content increases, while that of Mn(III) decreases with the increasing amount of Sr.

$La_{1-x}Sr_xMnO_3$ supported perovskite catalysts showed better performance of toluene oxidation than raw PG. The toluene conversion rate increases with the increasing amount of Sr when x = 0–0.3 and $La_{0.7}Sr_{0.3}MnO_3$ load on PG ranges from 3% to 11%. Toluene can be converted completely at 285 °C over 9% $La_{0.7}Sr_{0.3}MnO_3$/PG catalyst, and the change of catalyst activity is not obvious after addition of Sr. In the 100 h stability experiment of 9% $La_{0.7}Sr_{0.3}MnO_3$/PG catalyst, the toluene conversion rate was maintained above 95%.

ACKNOWLEDGEMENTS

This study was financially supported by the Natural Science Foundation of China (No. 41102023 and No. 41072036). The authors appreciate the financial support.

REFERENCES

[1] GROPPI G., CRISTIANI C., FORZATTI P., *Preparation, characterization and catalytic activity of pure and substituted La-hexaaluminate systems for high temperature catalytic combustion*, Appl. Catal. B, 2001, 35, 137.

[2] GRZYB K., MUSIALIK-PIOTROWSKA A., RUTKOWSKI J.D., *Methane combustion over monolithic catalysis*, Environ. Prot. Eng., 2006, 32, 5–10.

[3] CENTI G., CIAMBELLI P., PERATHONER S., RUSSO P., *Environmental catalysis: trends and outlook*, Catal. Today, 2002, 75, 3.

[4] DRAGO R.S., JURCZYK K., SINGH D.J., YOUNG V., *Low-temperature deep oxidation of hydrocarbons by metal oxides supported on carbonaceous materials*, Appl. Catal. B, 1995, 6, 155.

[5] PAPAEFTHIMIOUA P., IOANNIDESA T., VERYKIOS X.E., *Combustion of non-halogenated volatile organic compounds over group VIII metal catalysts*, Appl. Catal. B, 1997, 13, 175.
[6] MUSIALIK-PIOTROWSKA A., *Effect of platinum doping on activity of $LaMnO_3$ in oxidation of volatile organic compounds*, Environ. Prot. Eng., 2008, 34, 157.
[7] ZHOU J.C., WU D.F., JIANG W., LI Y.D., *Catalytic combustion of toluene over a copper–manganese–silver mixed-oxide catalyst supported on a wash coated ceramic monolith*, Chem. Eng. Technol., 2009, 32, 1520.
[8] LI J.F., YAN N.Q., QU Z., QIAO S.H., YANG S.J., GUO Y.F., LIU P., JIA J.P., *Catalytic oxidation of elemental mercury over the modified catalyst Mn/α-Al_2O_3 at lower temperatures*, Environ. Sci. Technol., 2010, 44, 426.
[9] SANZ O., ECHAVE F.J., SÁNCHEZ M., MONZÓN A., MONTES M., *Aluminium foams as structured supports for volatile organic compounds (VOCs) oxidation*, Appl. Catal. A, 2008, 340, 125.
[10] BERTINCHAMPS F., GRÉGOIRE C., GAIGNEAUX E.M., *Systematic investigation of supported transition metal oxide based formulations for the catalytic oxidative elimination of (choro)-aromatics*. *Part I. Identification of the optimal main active phases and supports*, Appl. Catal., B, 2006, 66, 1.
[11] SOLEYMANI M., MOHEB A., BABAKHANI D., *Hydrogen peroxide decomposition over nanosized $La_{1-x}Ca_xMnO_3$ ($0 \le x \le 0.6$) perovskite oxides*, Chem. Eng. Technol., 2011, 34, 49.
[12] LEVASSEUR B., KALIAGUINE S., *Effect of the rare earth in the perovskite-type mixed oxides $AMnO_3$ (A = Y, La, Pr, Sm, Dy) as catalysts in methanol oxidation*, J. Solid State Chem., 2008, 181, 2953.
[13] ROUSSEAU S., LORIDANT S., DELICHERE P., BOREAVE A., DELOUME J.P., VERNOUX P., *$La_{(1-x)}Sr_x$-$Co_{1-y}Fe_yO_3$ perovskites prepared by sol-gel method: Characterization and relationships with catalytic properties for total oxidation of toluene*, Appl. Catal., B, 2009, 88, 438.
[14] NITADORI T., KURIHARAM S., MISONO M., *Catalytic properties of $La_{1-x}A'_xMnO_3$ (A' = Sr, Ce, Hf)*, J. Catal., 1986, 98, 221.
[15] PONCE S., PEÑA M.A., FIERRO J.L.G., *Surface properties and catalytic performance in methane combustion of Sr-substituted lanthanum manganites*, Appl. Catal. B, 2000, 24, 193.
[16] MACHOCKI A., IOANNIDES T., STASINSKA B., GAC W., AVGOUROPOULOS G., DELIMARIS D., GRZEGORCZYK W., PASIECZNA S., *Manganese–lanthanum oxides modified with silver for the catalytic combustion of methane*, J. Catal., 2004, 227, 282.
[17] BATIS N.H., DELICHERE P., BATIS H., *Physicochemical and catalytic properties in methane combustion of $La_{1-x}Ca_xMnO_{3\pm y}$ ($0 \le x \le 1$; $-0.04 \le y \le 0.24$) perovskite-type oxide*, Appl. Catal. A, 2005, 282, 173.
[18] DENG J., ZHANG Y., DAI H., ZHANG L., HE H., AU C.T., *Effect of hydrothermal treatment temperature on the catalytic performance of single-crystalline $La_{0.5}Sr_{0.5}MnO_{3-\delta}$ microcubes for the combustion of toluene*, Catal. Today, 2008, 139, 82.
[19] DENG J.G., DAI H.X., JIANG H.Y., ZHANG L., WANG G.Z., HE H., AU C.T., *Hydrothermal fabrication and catalytic properties of $La_{1-x}Sr_xM_{1-y}Fe_yO_3$ (M = Mn, Co) that are highly active for the removal of toluene*, Environ. Sci. Technol., 2010, 44, 2618.
[20] CHEN T.H., XU H.F., PENG S.C., WANG J.Q., XU X.C., *Nanometer scale study on reaction of palygorskite with acid: reaction mechanism and change of specific surface area*, Geolog. J. Chin. Univ., 2004, 10, 98.
[21] SONG L., CHEN T.H., LI Y.X., LIU H.B., KONG D.J., CHEN D., *Performance of palygorskite supported Cu-Mn-Ce catalyst for catalytic oxidation of toluene*, Chin. J. Catal., 2011, 32, 652.
[22] LIU H.B., CHEN T.H., ZHANG X.L., LI J.H., CHANG D.Y., SONG L., *Effect of additives on catalytic cracking of biomass gasification tar over nickel-based catalyst*, Chin. J. Catal., 2010, 31, 409.
[23] LI J.H., ZHANG X.L., CHEN T.H., LIU H.B., SHI P.C., *Characterization and ammonia adsorption-desorption of palygorskite-supported manganese oxide as a low-temperature selective catalytic reduction catalyst*, Chin. J. Catal., 2010, 31, 454.

[24] CHEN T.H., XU X.C., YU S.C., *Nanometer mineralogy and geochemistry of palygorskite clays in the border of Jiangsu and Anhui provinces*, Chin. Sci. Press., Bei Jing, 2004.
[25] CHEN T.H., WANG J., QING C.S., PENG S.C., SONG Y.X., GUO Y., *Effect of heat treatment on structure, morphology and surface properties of palygorskite*, J. Chin. Ceram. Soc., 2006, 34, 1406.
[26] LI W.B., GONG H., *Recent progress in the removal of volatile organic compounds by catalytic combustion*, Acta. Phys. Chin. Sin., 2010, 26, 885.
[27] STEGE W.P., CADUS L.E., BARBERO B.P., *$La_{1-x}Ca_xMnO_3$ perovskites as catalysts for total oxidation of volatile organic compounds*, Catal. Today, 2011, 172, 53.
[28] MING C.B., YE D.Q., LIU Y.L., YANG L., *Effect of precious metal loaded on $LaMnO_3$ on catalytic oxidation of soot*, Chin. Environ. Sci., 2008, 29, 576.